$$u_{,xx}+\frac{1-\nu}{2}u_{,\phi\phi}+\frac{1+\nu}{2}v_{,x\phi}-\nu w_{,x}=0 \tag{1a}$$

$$\frac{1+\nu}{2}u_{,x\phi}+\frac{1-\nu}{2}v_{,xx}+v_{,\phi\phi}-w_{,\phi}=0 \tag{1b}$$

$$\nabla^4 w+12(R/h)^2(w-\nu u_{,x}-v_{,\phi})+4K^2\rho w_{,xx}=0 \tag{1c}$$

Where u, v, w are the nondimensional displacements, x, ϕ, the axial and circumferential nondimensional coordinates, L is the length of the shell, R its radius and h its thickness. ν is Poisson's ratio, $K^4=3(1-\nu^2)(R/h)^2$, and ρ is the ratio (eigenvalue) between the buckling stress and the classical buckling stress.

The SS4 boundary condition is

$$w=M_x=u=v=0 \quad \text{at} \quad x=0,\ L/R \tag{2}$$

Noting the similarity between the SS3 and the SS4 boundary conditions, the displacement field is taken in the form:

$$u=[U(x)+A\cos k\beta x]\cos n\phi \tag{3a}$$

$$v=[V(x)+B\sin k\beta x]\sin n\phi \tag{3b}$$

$$w=C\sin k\beta x\cos n\phi$$

where $\beta=\pi R/L$, k is the number of half waves in the axial direction, A, B, C, are constants and $U(x)$, $V(x)$, are to be regarded as correction functions.

Now, one can express A, B, in terms of C, and determine $U(x)$, $V(x)$, in such a way that Eqs. (1a) and (1b) together with the boundary conditions (2) will be satisfied. Details may be found in Refs. 5 and 6.

After the displacements (3a–c) have been determined up to the constant C, the Galerkin method (which is, in this case, equivalent to the Rayleigh-Ritz procedure) is applied to Eq. (1c)

$$\int_0^{2\pi}\int_0^{L/R}\left[\nabla^4 w+12\left(\frac{R}{h}\right)^2(w-\nu u_{,x}-v_{,\phi})+4K^2\rho w_{,xx}\right]w\,dx\,d\phi=0 \tag{4}$$

Performing the integration, yields

$$2\rho=Z+1/Z+\psi\theta \tag{5}$$

where

$$Z=[n^2+(k\beta)^2]^2/2K^2(k\beta)^2 \tag{6}$$

$$\theta=\frac{K^2}{\lambda^2}\frac{32}{(1+\nu)^2}\cdot\frac{[n^2-\nu(k\beta)^2]^2}{(n^2+(k\beta)^2]^4} \tag{7}$$

$$\psi=\begin{cases}\dfrac{t_n\lambda\cosh^2 t_n\lambda}{\dfrac{3-\nu}{1+\nu}\sinh 2t_n\lambda-2t_n\lambda} & \text{symmetric buckling, } k \text{ odd}\\[2ex] \dfrac{t_n\lambda\sinh^2 t_n\lambda}{\dfrac{3-\nu}{1+\nu}\sinh 2t_n\lambda+2t_n\lambda} & \text{antisymmetric buckling, } k \text{ even}\end{cases} \tag{8}$$

and

$$t_n^2=n^2/2K^2, \quad \lambda=[1/(2)^{1/2}][3(1-\nu^2)]^{1/4}L/(Rh)^{1/2} \tag{9}$$

In Eq. (5) the magnitude $Z+1/Z$ is recognized to be the expression for 2ρ at the SS3 boundary condition. The additional term $\psi\theta$ will be shown to be negligible. It is observed that Eq. (5) is an upper bound for the true value which is denoted by $2\rho^*$. A lower bound for $2\rho^*$ is that of the SS3 boundary condition as explained in Ref. 3. Hence

$$Z+1/Z<2\rho^*<Z+1/Z+\psi\theta \tag{10}$$

Since $t_n\lambda=(n/2)L/R$ one may replace, for usual shells, ψ by $[(1+\nu)/(3-\nu)]t_n\lambda/2$ in both the symmetrical and antisymmetrical buckling. Regarding Z as a continuous parameter, $Z+1/Z$ takes its minimum value for $Z=1$ which corresponds to $(k\beta)^2\approx 2K^2\gg n^2$. Substituting this value into Eq. (7), the result is

$$\psi\theta=\frac{4}{3(3-\nu)(1+\nu)(1-\nu^2)}\frac{nh^2}{RL}\frac{(\nu-t_n^2)^2}{(1+t_n^2)^4} \tag{11}$$

Hence, from Eq. (10),

$$2<2\rho^*<2+0(h^2/RL) \tag{12}$$

Thus, for all practical purposes, $\rho^*=1$ can be taken for the SS4 boundary condition. This is confirmed numerically by Ref. 7. Finally, it is noted that a result similar to Eq. (12) is obtained also in the axially symmetric buckling where $n=0$.

References

[1] Timoshenko, S. P. and Gere, J. H., *Theory of Elastic Stability*, 2nd ed., McGraw-Hill, New York, 1961.

[2] Hoff, N. J., "Low Buckling Stresses of Axially Compressed Circular Cylindrical Shells of Finite Length," *Journal of Applied Mechanics*, 1965, pp. 533–541.

[3] Hoff, N. J. and Rehfield, L. W., "Buckling of Axially Compressed Circular Cylindrical Shells at Stresses Smaller than the Classical Critical Value," *Journal of Applied Mechanics*, 1965, pp. 542–546.

[4] Donnell, L. H., "Stability of Thin Walled Tubes under Torion," Rept. 479, 1933, NACA.

[5] Baruch, M. and Harari, O., "Buckling of Cylindrical Shells with Axial Surface Tractions," *Journal of Applied Mechanics*, 1969, pp. 350–352.

[6] Durban, D., "On the Buckling of a Circular Cylindrical Shell under Non-uniform Load and Various Boundary Conditions," M.Sc. thesis, 1971 (in Hewbrew), Technion, Israel Instute of Technology, Haifa, Israel; also TAE Rept. 142, to be published.

[7] Hoff, N. J. and Soong, T. C., "Buckling of Circular Cylindrical Shells in Axial Compression," *Int. S. Mech. Sci.*, 7, 1964, pp. 489–520.

Calculations of the Turbulent Boundary Layer in Supersonic Nozzles

E. R. BERGSTROM* AND S. RAGHUNATHAN†

Loughborough University of Technology, Loughborough, England

Nomenclature

a	= speed of sound
A^*	= throat area
$A(x)$	= area of a cross section a distance x from the throat
C_f	= local skin-friction coefficient
g_w	= normalized wall enthalpy h_w/h_o
H	= form factor $\delta^*(x)/\theta$
H_i	= incompressible flow form factor
j	= 0, 1 for two-dimensional and axisymmetric flow, respectively
L	= length of the nozzle
M_e	= Mach number at the edge of the boundary layer
$M_e(x)$	= average Mach number in the potential core at a section a distance x from the throat
M_{eL}	= measured nozzle exit Mach number
$M_b(x)$	= one-dimensional flow Mach number based on the physical boundary at a distance x from the throat
M_{bL}	= nozzle exit value of $M_b(x)$
R	= radius of the axisymmetric body
T	= temperature
$\tilde{T}$	= reference temperature
x	= coordinate along the body surface
γ	= ratio of specific heats (taken as 1.4 for air)
$\delta^*(x)$	= boundary-layer displacement thickness at a section a distance x from the throat
θ	= boundary-layer momentum thickness
Θ	= transformed momentum thickness $\theta(T_e/T_o)^{(\gamma+1)/(2(\gamma-1)}$
μ	= coefficient of viscosity
$\tilde{\mu}$	= viscosity evaluated at the reference temperature

Received November 29, 1971; revision received January 25, 1972.

Index categories: Boundary Layers and Convective Heat Transfer—Turbulent; Supersonic and Hypersonic Flow; Nozzle and Channel Flow.

* Lecturer, Department of Transport Technology.

† Mature Research Student, Department of Transport Technology.

ν = kinematic viscosity
σ = Prandtl number

Subscripts

e = local external flow conditions
w = local wall surface conditions
o = freestream stagnation conditions

Introduction

RECENTLY a method for analysing the compressible turbulent boundary layer with pressure gradient and heat transfer was given by Sasman and Cresi.[1] This method is an improvement over most previous analyses in that it is reasonably accurate for wide ranges of positive and negative pressure gradients. For a solution the method requires the flow Mach number distribution as an input, which for internal flows containing thick boundary layers is not known a priori. In this Note, three methods are proposed for analyzing the boundary layers in supersonic nozzles. The first method applies a linear correction to the Mach number distribution given by the one-dimensional area ratio, and the second, a linear correction for the boundary-layer displacement thickness. In the solutions presented here, known values of the nozzle exit Mach numbers are employed, but the methods will readily form the basic calculation in an iterative procedure for determining an unknown Mach number distribution starting with an approximate value of the exit Mach number. In the third method, a differential equation for the Mach number gradient is formulated and solved simultaneously with the differential equations for the momentum and moment of momentum. The unique advantage of the third method is that it does not require the nozzle Mach number distribution as an input.

Basic Differential Equations

The differential equations for the momentum thickness θ and form factor H are given by,[1]

$$\frac{df}{dx} = 1.268\left[\left(-\frac{f}{M_e}\right)\left(\frac{dM_e}{dx}\right)(1+g_w H_i)-\frac{jf}{R}\left(\frac{dR}{dx}\right)+A1\right] \tag{1}$$

$$\frac{dH_i}{dx} = -\frac{1}{2M_e}\left(\frac{dM_e}{dx}\right)H_i(H_i+1)^2(H_i-1)\times \left[1+(g_w-1)\frac{H_i^2+4H_i-1}{(H_i+1)(H_i+3)}\right]+\frac{(H_i^2-1)A1}{f}\times \left[H_i-\frac{0.011\,(H_i+1)(H_i-1)^2}{H_i^2}\left(\frac{2}{C_f}\right)\frac{T_o}{\bar{T}}\right] \tag{2}$$

where

$$A1 = 0.123e^{-1.561H_i}(M_e a_o/\nu_o)\left(\frac{T_e}{\bar{T}}\right)\left(\frac{T_e}{T_o}\right)^3\left(\frac{\bar{\mu}}{\mu_o}\right)^{0.268} \tag{3}$$

$$f = (M_e\, a_o\,\Theta/\nu_o)^{1.268} \tag{4}$$

$$\Theta = \theta/(T_o/T_e)^{(\gamma+1)/2(\gamma-1)} \tag{5}$$

$$H_i = (1/g_w)\{H-[(\gamma-1)/2]M_e^2\}/\{1+[(\gamma-1)/2]M_e^2\} \tag{6}$$

$$C_f = 0.246e^{-1.561H_i}(M_e a_o\Theta/\nu_o)^{-0.268}(T_e/\bar{T})(\bar{\mu}/\mu_o)^{0.268} \tag{7}$$

$$\bar{T}/T_o = 0.5\,T_w/T_o+0.22\sigma^{1/3}+(0.5-0.22\sigma^{1/3})(T_e/T_o) \tag{8}$$

Linear Correction for Mach Number

Assuming a linear correction for Mach number to the one-dimensional area ratio value, the true I-D flow Mach number distribution can be approximated by

$$M_e(x) = M_b(x)-(M_{bL}-M_{eL})(x/L) \tag{9}$$

Thus, when $x = 0$, $M_e(0) = M_b(0) = 1.0$, and when $x = L$, $M_e(L) = M_{eL}$, the measured value. Knowing the Mach number distribution from Eq. (9), Eqs. (1) and (2) can be solved using the approximation $M_e = M_e(x)$ to obtain the boundary-layer characteristics of any nozzle. The above approximation for Mach number in Eqs. (1) and (2) is used in all subsequent analyses.

A partial test for the validity of the method is to compare the measured Mach number distribution with that inferred from the calculated displacement thickness distribution. Complete verification of the method requires a comparison between measured values of skin-friction coefficient and momentum thickness and predicted values.

Linear Correction for the Displacement Thickness

A linear correction for displacement thickness to the physical contour can be assumed instead of a linear correction for Mach number. With this assumption the Mach number distribution can be expressed as

$$\frac{A(x)-2\pi R\,\delta^*(x)}{A^*} = \frac{1}{M_e(x)}\left[\frac{2+(\gamma-1)M_e(x)^2}{\gamma+1}\right]^{(\gamma+1)/2(\gamma-1)} \tag{10}$$

where

$$\delta^*(x) = \delta_L{}^*(x/L) \tag{11}$$

Here $\delta_L{}^*$ is the boundary-layer displacement thickness at the nozzle outlet and is given by the difference between the physical radius and the radius corresponding to the one-dimensional area based on the measured exit Mach number. The Mach number distribution can be obtained from Eqs. (10) and (11).

When the correction for δ^* is applied to the entire length of a contoured nozzle it leads to a decreasing core area and Mach number towards the exit section. This occurs when the incremental increase in $\delta^*(x)$ from one axial position to another is greater than the incremental change in the nozzle radius. Therefore, the full correction is applied over a reduced length $\bar{L}$, which is the distance from the throat to the cross section where the above occurs, a constant value of $\delta^*(x) = \delta_L{}^*$ then being applied up to the exit plane. $\bar{L}$ can be obtained by initially applying the correction over the entire length L and noting the point where the core area starts to decrease. The boundary-layer characteristics of a nozzle can be obtained by solving Eqs. (10) and (11) together with Eqs. (1) and (2). Again the validity of the method is checked against experimental results.

Three Equations Method

The two methods described above are based on the two basic differential Eqs. (1) and (2) and the various auxiliary equations listed. They need the measured exit Mach number for a non-iterative solution. This restriction and the resultant approximations can be dispensed with, by formulating a third differential equation for the Mach number gradient. This is a method in which the two equations of motion, namely momentum and moment of momentum, are combined with what is essentially the equation of continuity for ducted flows, Eq. (10). This can be differentiated to give an equation of the form

$$dM_e(x)/dx = f_1[M_e(x),\ H_i,\ f,\ dH_i/dx,\ df/dx] \tag{12}$$

In functional form, Eqs. (1) and (2) become

$$df/dx = f_2(M_e,\ dM_e/dx,\ H_i,\ f) \tag{13}$$

$$dH_i/dx = f_3(M_e,\ dM_e/dx,\ H_i,\ f) \tag{14}$$

combining Eqs. (12–14) and writing $M_e \simeq M_e(x)$ yields

$$dM_e(x)/dx = f_4[M_e(x),\ H_i,\ f] \tag{15}$$

$$df/dx = f_5[M_e(x),\ H_i,\ f] \tag{16}$$

$$dH_i/dx = f_6(M_e(x),\ H_i,\ f) \tag{17}$$

Thus, Eqs. (15–17) can be solved simultaneously for $M_e(x)$, f and H_i by means of the Runge-Kutta numerical integration technique. The full forms of these equations are long algebraically and can be found elsewhere.[2]

Results and Discussion

Figure 1 shows the Mach number distribution as calculated by the three equations method for the Caltech Mach 4 conical nozzle. Only the one distribution is shown as the results of all three analyses coincided. The experimentally measured Mach

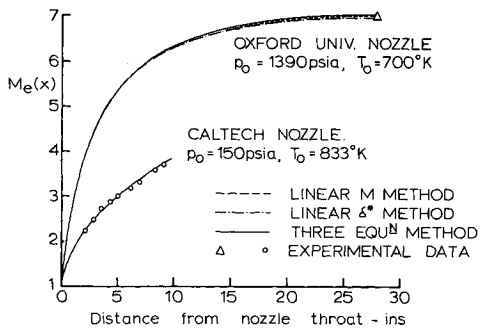

Fig. 1 Comparison of calculated and experimental nozzle Mach numbers.

numbers[3] are shown for comparison. The difference between the experimental and the theoretical results within the nozzle can be attributed to the fact that the measured value is the Mach number at the edge of the boundary layer, whereas because of the use of Eqs. (9, 10 and 12), the theories predict an average value of the Mach number at a cross section. In practice in an expanding supersonic flow $M_e(x) \gtrsim M_e$, as shown by the results. The exit values of the Mach number are in good agreement. Also in Fig. 1 are shown the calculated and experimental Mach numbers for the Oxford University Mach 7 contoured nozzle.[4] Again the differences between the three methods are negligible. It is interesting to note that the values of the exit Mach number predicted by the three equations method for both the nozzles are in close agreement with the experimental values.

Figure 2 shows the variation of the Mach number and boundary-layer characteristics at the exit of the contoured nozzle with the wall to stagnation enthalpy ratio and the freestream unit Reynolds number. These calculations were made with the three equations method. It is seen that the Mach number and boundary-layer characteristics change significantly with changes in the wall temperature and total pressure, contrary to practice in which it is often assumed that the exit Mach number, and hence δ^*, remains constant with changes in driver conditions. Comparison of the predicted and experimental values of C_f and θ have not been made due to a lack of experimental data.

Conclusions

1) The three methods proposed for calculations of the compressible turbulent boundary layer in supersonic nozzles are in close agreement with each other and the experimental results for exit Mach number and displacement thickness. 2) The appreciable variations in the boundary-layer characteristics of nozzles with inlet total pressure and nozzle wall temperature can be readily predicted by the three equations method.

References

[1] Sasman, P. K. and Cresci, R. J., "Compressible Turbulent Boundary Layer with Pressure Gradient and Heat Transfer," *AIAA Journal*, Vol. 4, No. 1, Jan. 1966, pp. 19–25.

[2] Bergstrom, E. R. and Raghunathan, S., "Calculations of the Compressible Turbulent Boundary Layer with Pressure Gradient and Heat Transfer in Internal Flows with Particular Reference to Supersonic Nozzles," TT7104, June 1971, Loughborough University of Technology, England.

[3] Back, L. H. and Cuffel, R. F., "Relationship Between Temperature and Velocity Profiles in a Turbulent Boundary Layer Along a Supersonic Nozzle with Heat Transfer," *AIAA Journal*, Vol. 8, No. 11, Nov. 1970, pp. 2066–2069.

[4] Lagraff, J. E., "Comparative Transition Measurements on a Hollow Cylinder Model," ARC 31233, Hyp. 755, Aeronautical Research Council, England.

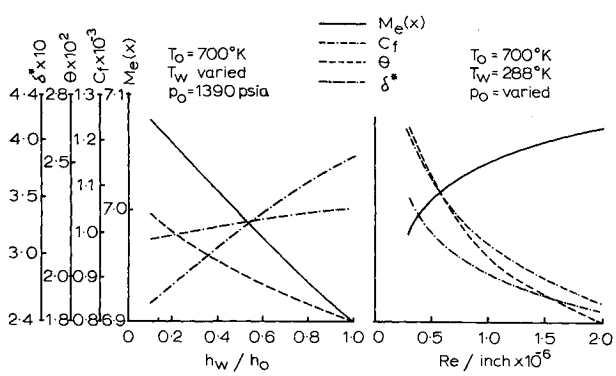

Fig. 2 Variation in nozzle flow parameters with enthalpy ratio and unit Reynolds number.

Binary Diffusion of a Jet Embedded in a Boundary Layer

F. D. HAINS* AND A. J. BAKER†
Bell Aerospace Division of Textron, Buffalo, N.Y.

In some recent studies[1–3] of the penetration and mixing of a hydrogen jet injected normal to a supersonic airstream, the jet turns and remains within the boundary layer. Because of the shape of the boundary-layer velocity profile, the curves of constant concentration form a "Mexican hat" shape as shown in Fig. 1. In this Note, a theoretical model based on the binary diffusion equation is presented along with numerical solution of the governing equation by the method of finite elements.

The dimensionless form of the binary diffusion equation for species A is[4]

$$\vec{V} \cdot \nabla \omega_A = D[\nabla^2 \omega_A + \rho^{-1}(\nabla \rho \cdot \nabla \omega_A)] \tag{1}$$

where ρ is the mixture density, $\vec{V}$ is the fluid velocity, and ω_A is the mass fraction of species A. The diffusivity D is assumed to be constant in Eq. (1). All dimensionless quantities are referenced with respect to the freestream conditions at the first station in x and the characteristic length is chosen so that calculations begin at $x = 1$.

The mixture density is assumed to satisfy the perfect gas law in the dimensionless form

$$\rho = GM/M_B \tag{2}$$

where $G = p/T$. The quantities p and T are the dimensionless pressure and temperature, respectively, and M and M_B are the

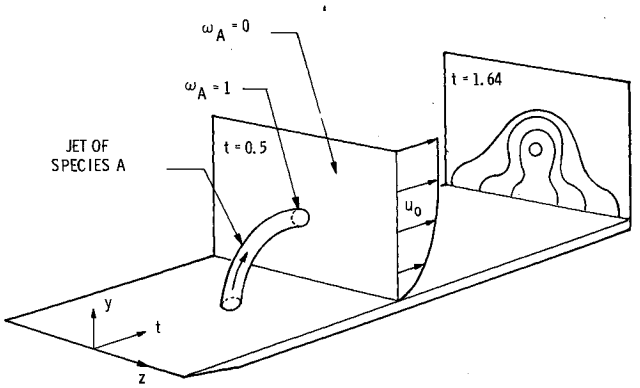

Fig. 1 Diffusion of a jet embedded in a boundary layer.

Received December 6, 1971.

* Principal Scientist, Advanced Technology Research.
† Principal Scientist, Continuum Mechanics Research. Associate Member AIAA.